EasyChair Preprint

№ 2738

Band Gap Tailoring of Cu2Se by Chlorine: A First Principles Study

Zeesham Abbas, Iqra Iftikhar and Sikander Azam

February 21, 2020

Band Gap Tailoring of Cu_2Se by Chlorine: A First Principles Study

Zeesham Abbas[1], Iqra Iftikhar[1], Sikander Azam[*2]

[1]Department of Physics, The University of Lahore, Sargodha Sub-Campus, 40100, Pakistan

[2]Faculty of Engineering and Applied Sciences, Department of Physics, RIPHAH International University I-14 Campus Islamabad, Pakistan

***Corresponding: Sikander.azam@gmail.com**

ABSTRACT

The main objective of this work is the prediction of optoelectronic properties of Cl doped Cu2Se by FP-(L)APW method which is implemented in WIEN2k code. The structure is optimized by using GGA as exchange-correlation functional. TB-mBJ (Tran-Bhala modified Becke-Johnson) approximation was used for the prediction of the electronic properties of this compound and this choice is motivated by its proven success for this kind of study. The electronic properties have shown the metallic nature. The optoelectronic transitions between the valence band top and the conduction band bottom have been identified by an analysis of the real and imaginary part variations of the dielectric function.

Keywords: FP-(L)APW method; WIEN2k code; Optoelectronic properties.

INTRODUCTION

Copper chalcogenides have been compounds of extreme interest for researchers in recent past due to their potential applications in thermoelectric and photovoltaic devices [1, 2]. As an example, cuprous chalcogenide (Cu_2Se) have wide applications in thermoelectric generators [3], solar cells [4, 5] and optoelectronic devices [6, 7]. In particular, an important ingredient in CIGS ($Cu(In,Ga)Se_2$ solar cells) is Cu_2Se, which is among the most promising technologies in the field of renewable energy. Regardless of its significant applications and simple chemical formula, the atomic structure of Cu_2Se in low-temperature phase was undefined until recent past, which hindered the theoretical calculations of the physical properties of Cu_2Se. Definitely, some DFT studies are available in the literature that are based on high temperature phase of Cu_2Se [8, 9], which shows huge difference between the experimental and theoretical results. With the help of

X-ray diffraction calculations, a complex monoclinic structure of Cu_2Se was by Gulay *et al.* for low-temperature phase [10]. Nguyen *et al.* used genetic algorithm study to predict a naiver layered structure of Cu_2Se [11], and approximately at the same time a similar layered structure was detected experimentally [7]. Layered configuration is found to be one of the most stable dynamical structural model [11].

Layered nature of the transition metal chalcogenides is attracting the interest of researchers as they have been emerging as potential candidates to be utilized in future nano-scale devices [12]. In fact, van der Waals (vdW) forces of attractive nature weakly bound their layered structures, permitting the trite segregation of the layered building blocks and resultant applications of their interesting two-dimensional characteristics in different areas of material science [12]. Newly proposed model of Cu_2Se is shown in Fig. 1 having strongly bonded layered building blocks that contain six atomic layers [11].

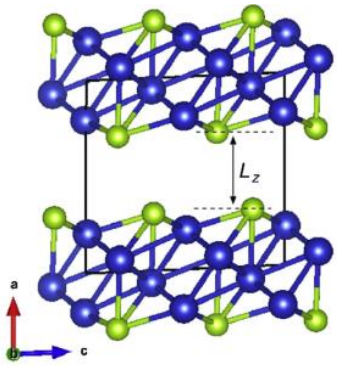

Fig. 1: Layered structure of Cu_2Se

Values of energy band gap measured in optical experiments are between 1.0 to 1.3 eV [13-15]. In contrast, cubic models of Cu_2Se having semi-metallic and metallic nature were reported in earlier first-principles studies [8, 9]. Several experimental attempts have been made in order to determine crystal structure of Cu_2Se in low-temperature phase. However, main focus of many experimental studies was to determine lattice parameters instead of detailed atomic positions. It is important to note that layered structure of Cu_2Se at low temperature show considerable low value of energy band gap (0.74 eV) as calculated by meta-GGA method [11]. However, it is uncertain that whether these discrepancies between different theories comes out due to the use of different structural models, as earlier studies were carried out by employing different computational

methods having different accuracies. Therefore, such discrepancies must be addressed through further theoretical studies.

In this study, by using first-principles calculations in the framework of density functional theory by employing GGA approximation, we calculated electronic and optical properties of Cu_2Se and [Cu_2Se]:Cl. These studies give more explanation regarding physical properties of the photovoltaic materials based on Cu_2Se.

COMPUTATIONAL DETAILS

In this article, WIEN2k package is used with the FP-LAPW (full-potential augmented plane wave) method for the analysis of significant properties of Cu_2Se and [Cu_2Se]:Cl [16]. We used newly developed TB-mBJ (Tran-Bhala modified Becke-Johnson) and optimized values of lattice parameters for calculation of essential exchange-correlation potentials [17]. In FP-LAPW method, two regions are combined to form space of unit cell i.e. (a) IR (interstitial region) and (b) muffin-tin (atomic spheres). Potential is taken as constant in interstitial region whereas in muffin-tin region it is taken as a function of $r \leq R_{MT}$ (R_{MT} = Muffin-tin radius) and is spherically symmetric. No leakage of current is ensured from the core states of atoms by choosing suitable values of muffin-tin radii for different elements and no overlapping of the atomic spheres exist in the convergence of total energy. Plane wave function and radial wave function time's spherical harmonics are used to solve SWE (Schrodinger wave equation) in interstitial region and muffin-tin region, respectively.

The value of maximum angular momentum (l_{max}) is taken as 10 to expand wave functions in muffin-tin radii and value of cutoff energy is set to be -6.0 Ry. The values for convergence point of total energy and force are taken as 0.0001 Ry and 0.001 Ry/au, respectively. To achieve these values a k-mesh of 500 points has been taken and the cutoff parameter for plane wave i.e. $R_{MT}*K_{max}$ and G_{max} are taken as 7.0 and 12, respectively, in first Brillouin zone. Where R_{MT} and K_{max} are the values of smallest muffin-tin radius and largest reciprocal lattice vector, respectively. Forces on the atoms are reduced to less than 1mRy/au in order to get relaxed geometry for the calculations. Unit cells of Cu_2Se and Cu_2Se are shown in Fig. 1 (a) and (b), respectively.

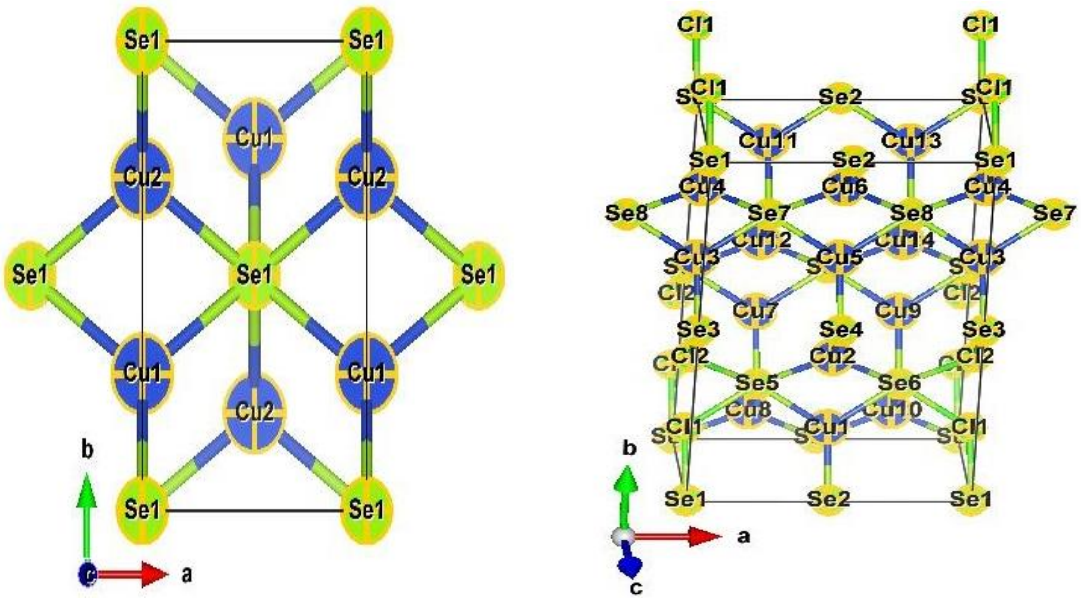

(a) (b)

Fig. 2: Unit cell structures of (a) Cu_2Se (b) [Cu_2Se]:Cl

RESULTS AND DISCUSSION

ELECTRONIC PROPERTIES

Information regarding the optoelectronic properties of the material under is mainly provided by the density of states (DOS) and energy band structure. In this section of the manuscript, electronic properties of Cu_2Se and [Cu_2Se]:Cl are discussed by using the calculated results of band space dispersion, electronic density of states and partial density of states (PDOS). Partial density of states (PDOS) are useful in the explanation of the contributions from different components of angular momentum and are also helpful for the explanation of the origin of sub energy bands.

BAND STRUCTURE

Properties like energy band gaps and energy band structures play an important role while deciding an efficient semiconductor material for applications in electronic devices. In this section of the article we discussed the calculated energy band structure of Cu_2Se and [Cu_2Se]:Cl. Calculated energy band structures along highly symmetric points of the first Brillouin zone are shown in Fig. 3. Band structures are plotted for the range of -5.0 to 5.0 eV. Cu_2Se is direct band gap material as VBM (valance band maxima) and CBM (conduction band minima) are collinear

at Γ whereas [Cu_2Se]:Cl possess indirect band gap as VBM and CBM are not present at same point. It can be noted from Fig. 3 that values of energy band gap are 0.824 and 0.145 eV for Cu_2Se and [Cu_2Se]:Cl, respectively.

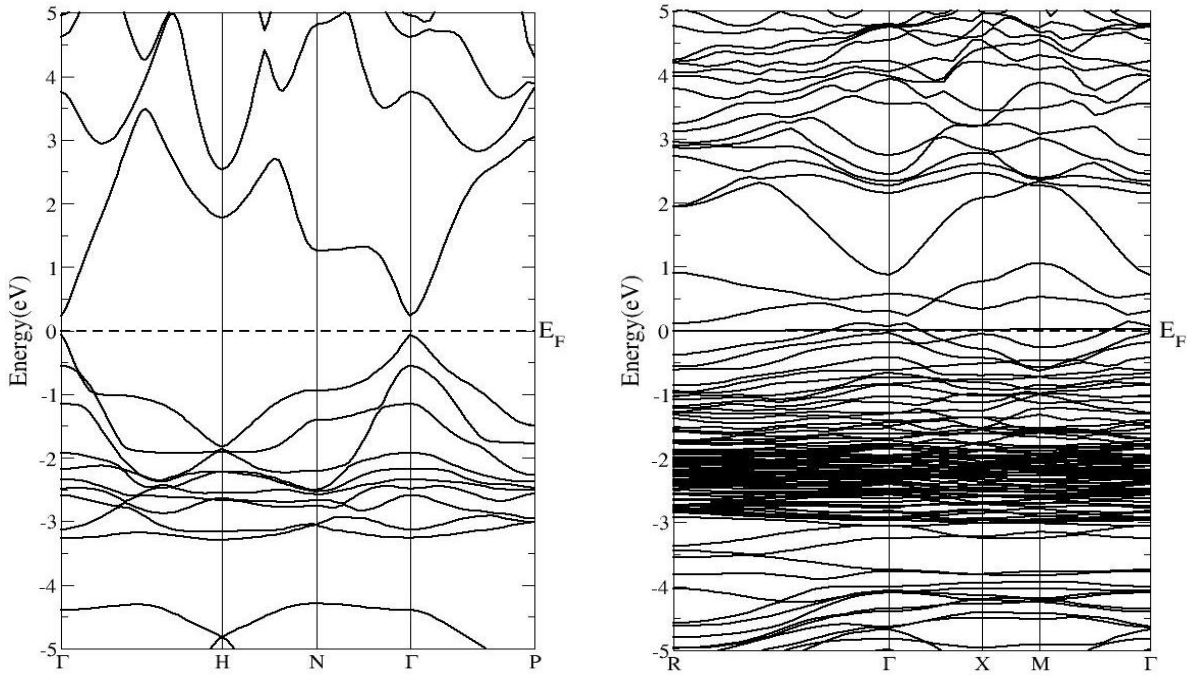

(a) (b)

Fig. 3: Band structures of (a) Cu_2Se (b) [Cu_2Se]:Cl

DENSITY OF STATES

Contribution of different electronic states in electronic and optical properties of Cu_2Se and [Cu_2Se]:Cl have been studied in VB and CB by calculating partial density of states (PDOS) and total density of states (TDOS) in this section of the article. PDOS and TDOS are calculated for foresaid compounds at stable lattice parameters by using mBJ-GGA approximation. Calculated DOS are presented in Fig. 4 (a) and (b) for Cu_2Se and [Cu_2Se]:Cl, respectively. One can clearly see that Fig. 4 (a) is divided into three portions in bottom up mode i.e. (i) TDOS and PDOS of elements, (ii) PDOS of Cu and (iii) PDOS of Se. Total and partial density of states for Cu_2Se are plotted for the energy range of -6.0 to 6.0 eV with Fermi level at 0 eV. Contributions from different sub-shells of the atoms in a compound can be explained by calculating PDOS of that compound. We can divide the valance band in the plots of TDOS and PDOS into two sections i.e. section 1 from -6.0 to -4.0 eV and section 2 from -4.0 to 0 eV. It can be observed from Fig. 4 (a) that in

section 1 of the valance band both Cu and Se have approximately same contributions whereas the plots of PDOS shows that in this section major contributions comes from Se-p orbitals and some minor contributions are also present due to Cu-d orbitals. In section 2, major contributions comes from Cu atoms and Se atoms have no impact in this section. From the plots of PDOS, it can be noted that major contributions in this section are due to Cu-d and Se-p orbitals. Similarly, it can be noticed from the plot of TDOS that in conduction band both atoms have approximately same impact. However, it can be observed from the plots of PDOS that Se-S, Se-p and Cu-d orbitals have major contribution at lower energies whereas at energies higher than 3.0 eV, Se-p, Se-d and Cu-d orbitals have major contributions.

One can clearly see that Fig. 4 (b) is divided into four portions in bottom up mode i.e. (i) TDOS and PDOS of elements, (ii) PDOS of Cl, (iii) PDOS of Cu and (iv) PDOS of Se. Total and partial density of states for [Cu_2Se]:Cl are plotted for the energy range of -8.0 to 8.0 eV with Fermi level at 0 eV. We can divide the valance band in the plots of TDOS and PDOS into two sections i.e. section 1 from -8.0 to -4.0 eV and section 2 from -4.0 to 0 eV. It can be observed from Fig. 4 (b) that in section 1 of the valance band both Cl, Cu and Se have approximately same contributions whereas the plots of PDOS shows that in this section major contributions comes from Se-p and Cl-p orbitals and some minor contributions are also present due to Cu-d orbitals. In section 2, major contributions comes from Cu atoms but Se and Cl atoms also have some minor contributions in this region. From the plots of PDOS, it can be noted that major contributions in this section are due to Cu-d and some minor contributions due to Se-p and Cl-p orbitals are also present. Similarly, it can be noticed that valance band can also be divided into two regions i.e. section 1 from 0 to 4.0 eV and section 2 from 4.0 to 8.0 eV. In section 1 of the conduction band, major contributions are due to Se atoms whereas some minor contributions are also present due to Cu atoms whereas the plots of PDOS shows that in this section major contributions comes from Se-p and Cu-d orbitals and some minor contributions are also present due to Se-s and Se-d orbitals. In section 2, major contributions comes from Se and Cl atoms. From the plots of PDOS, it can be noted that major contributions in this section are due to Se-d, Se-p and Cu-s orbitals whereas some minor contributions due to Cu-d orbitals are also present.

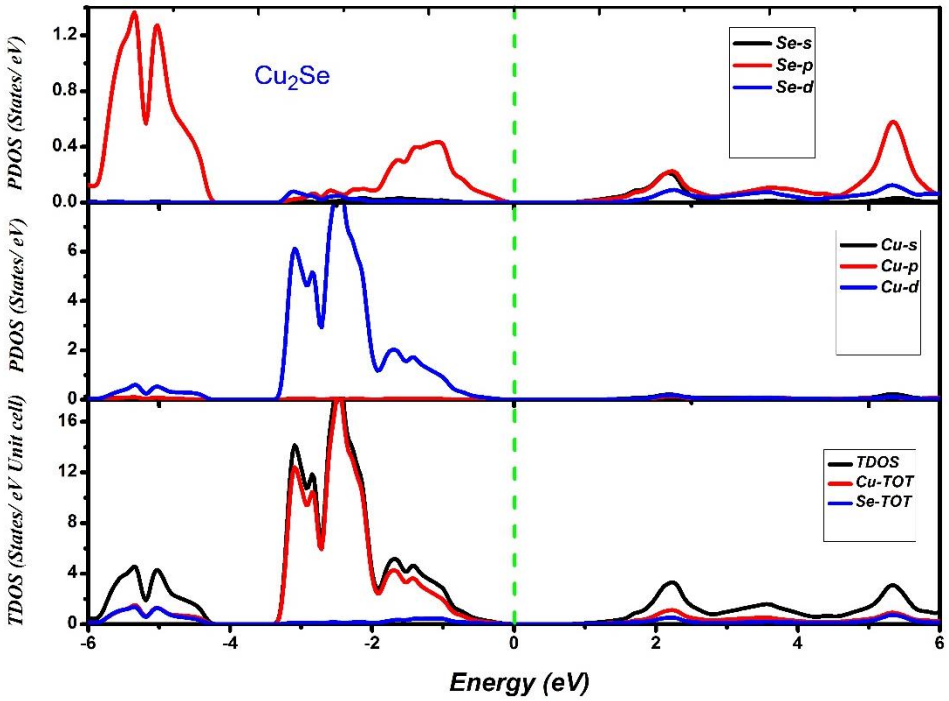
Cu2Se
Se-s
Se-p
Se-d
Cu-s
Cu-p
Cu-d
TDOS
Cu-TOT
Se-TOT
PDOS (States/ eV)
PDOS (States/ eV)
TDOS (States/ eV Unit cell)
Energy (eV)

(a)

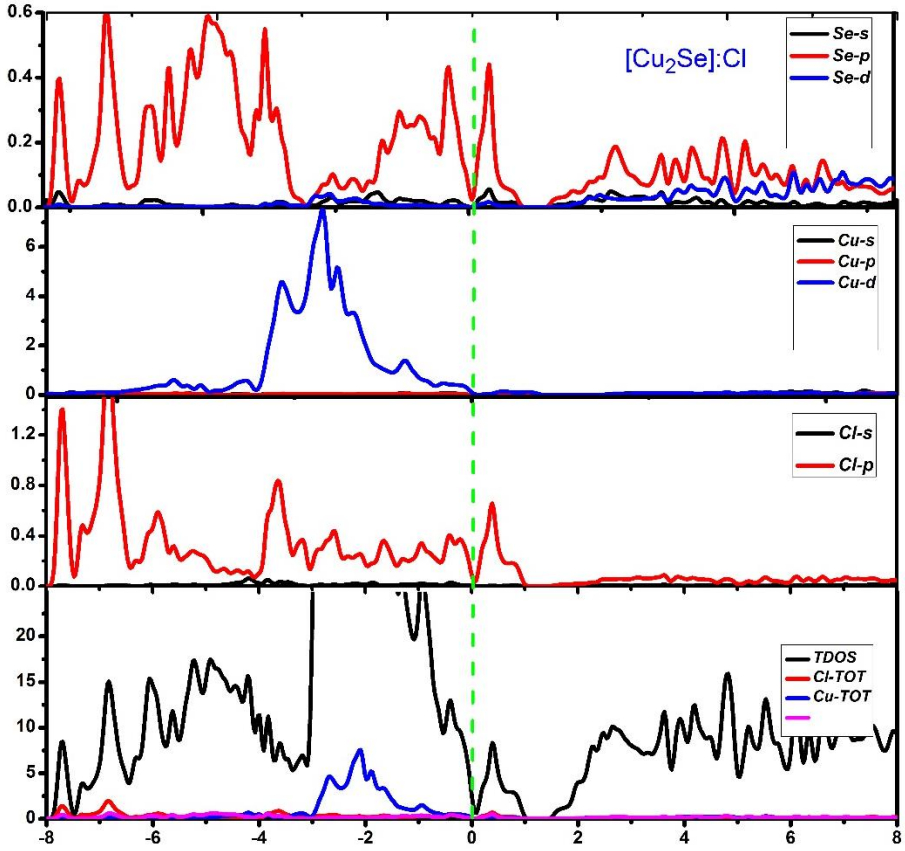
[Cu2Se]:Cl
Se-s
Se-p
Se-d
Cu-s
Cu-p
Cu-d
Cl-s
Cl-p
TDOS
Cl-TOT
Cu-TOT

(b)

Fig. 4: Total and partial density of states for (a) Cu_2Se (b) [Cu_2Se]:Cl

OPTICAL PROPERTIES

Calculated optical properties such as dielectric function, extinction coefficient, refractive index, absorption coefficient, energy loss function and optical conductivity for Cu_2Se and [Cu_2Se]:Cl are discussed in this section in order to get deeper understanding of the electronic structure. Appropriate knowledge regarding refractive index and absorption coefficient is the primary requirement in order to design effective optoelectronic devices. These theoretical results are in good agreement with previously reported experimental as well as theoretical results. Optical properties of aforementioned compounds are explained by taking average of the parameters along three axis as these compounds possess tetragonal symmetry. Calculated results of the optical parameters are shown in Fig. 5 (a-g).

Complex dielectric function can be used to explain the optical response of the semiconductor material over the energy range of 0-14 eV. Dielectric function can be calculated by using the following equation:

$$\varepsilon(\omega) = \varepsilon_1(\omega) + i\varepsilon_2(\omega) \tag{1}$$

Where $\varepsilon_2(\omega)$ and $\varepsilon_1(\omega)$ are the imaginary and real parts of the complex dielectric function, respectively. Imaginary part $\varepsilon_2(\omega)$ of dielectric function describes all probable excitations of electrons between occupied and unoccupied states whereas all the stored energies in material are associated with real part $\varepsilon_1(\omega)$ of the complex dielectric function. Imaginary part $\varepsilon_2(\omega)$ of dielectric function can be calculated by using the following relation [18]:

$$\varepsilon_2(\omega) = \frac{Ve^2}{2\pi m^2\omega^2}\int d^3k \sum_{n,n'}\langle k,n|p|k,n'\rangle^2 f(kn)[1-f(kn')]\,\delta(E_{kn}-E_{kn'}-\omega) \tag{2}$$

Where m, e, $f(kn)$ and E_{kn} are used to specify mass of electron, charge of electron, Fermi distribution function and eigenvalue of the n^{th} state wave function of the crystal $|k,n\rangle$, respectively. And p represents the momentum matrix elements between states n and n'. The real part $\varepsilon_1(\omega)$ of dielectric function can be calculated by using the following Kramer-Kronig relation [19, 20]:

$$\varepsilon_1(\omega) = 1 + \frac{2}{\pi}\int_0^{\infty}\frac{\varepsilon_2(\omega)\omega' d\omega'}{\omega'^2-\omega^2} \tag{3}$$

Calculated results of the real part $\varepsilon_1(\omega)$ of dielectric function are presented in Fig. 5 (a). One can see that peaks are shifted towards lower energies and static value also increases by the doping of chlorine in Cu_2Se. Highest values in the spectra of real part $\varepsilon_1(\omega)$ of complex dielectric function occurs at approximately 1.0 and 0.5 eV for Cu_2Se and [Cu_2Se]:Cl, respectively. There is a sharp decrease in the spectra of $\varepsilon_1(\omega)$ for [Cu_2Se]:Cl after the peak value. Spectra of Cu_2Se and [Cu_2Se]:Cl enters in the negative region at approximately 4.3 and 7.4 eV, respectively, that shows metallic response of the compounds for higher frequencies of the incident photons. An important physical parameter of the material is the value of its static dielectric function $\varepsilon_1(0)$. It can be observed from Fig. 5 (a) that static values of dielectric constant $\varepsilon_1(0)$ are almost 12.6 and 22.4 for Cu_2Se and [Cu_2Se]:Cl, respectively. Following Penn relation can be used to relate the static value $\varepsilon_1(0)$ of complex dielectric function and energy band gap (Eg) [21]:

$$\varepsilon_1(0) = 1 + \left(\frac{\hbar\omega_p}{E_g}\right)^2 \tag{4}$$

Calculated spectra of imaginary part $\varepsilon_2(\omega)$ of dielectric function for Cu_2Se and [Cu_2Se]:Cl are presented in Fig. 5 (b). One can see that peaks are shifted towards lower energies by the doping of chlorine in Cu_2Se but overall profile of the spectra is almost similar for both compounds. From Fig. 5 (b), it can be observed that main peaks for Cu_2Se and [Cu_2Se]:Cl are present in the energy range of 2.0 to 8.0 eV and 0 to 5.0 eV, respectively. HOMO-LUMO transitions between different orbitals of VB and CB are responsible for these peaks in the said energy regions. Highest peaks are present at 4.3 and 0.7 eV in the spectra of Cu_2Se and [Cu_2Se]:Cl, respectively. For energies higher than 8.0 eV both compounds shows maximum reflectivity and negligible absorption of incident photons is present in this region.

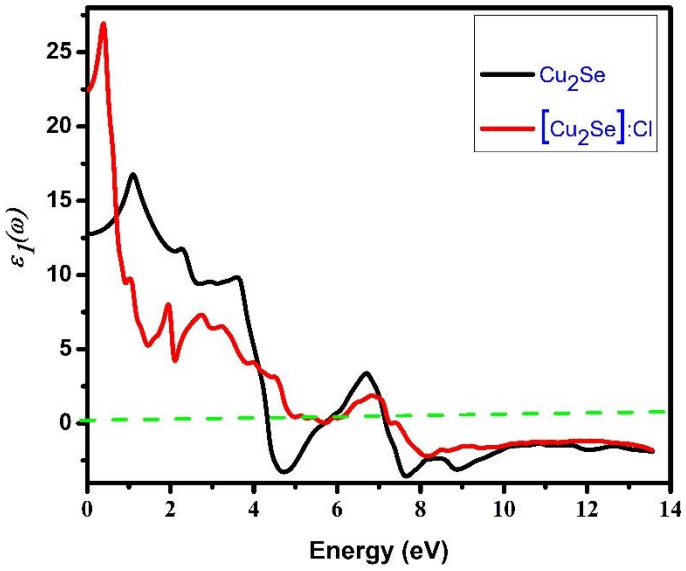

(a)

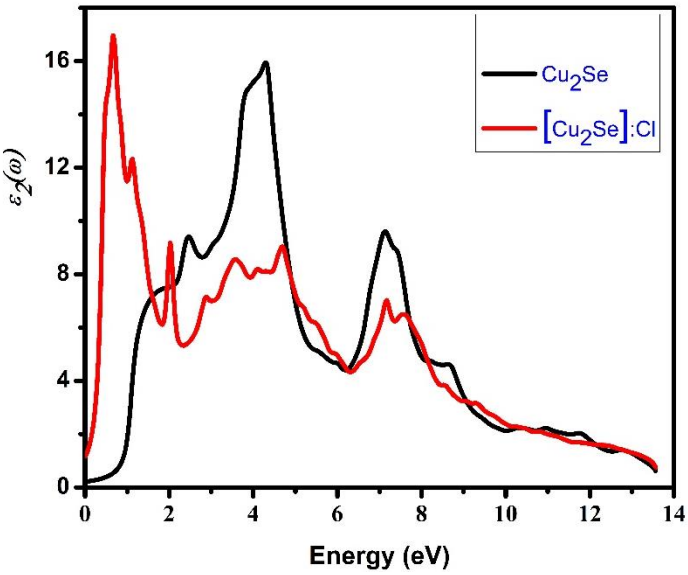

(b)

Refractive index $n(\omega)$, also known as the material transparency is the measure of the speed with which light can through that material whereas extinction coefficient $k(\omega)$ specifies the loss of energy during the propagation of photons through the medium. Refractive index $n(\omega)$ is an important quantity to be calculated in order to manufacture effective optoelectronic devices such as wave guides, detectors, photonic crystals and solar cells. Obviously, extinction coefficient $k(\omega)$ and refractive index $n(\omega)$ shows similar pattern as that of the imaginary part $\varepsilon_2(\omega)$ and real part

$\varepsilon_1(\omega)$ of complex dielectric function, respectively. Complex refractive index can be calculated by using the following equation [22]:

$$\tilde{n}(\omega) = n(\omega) + ik(\omega) \tag{5}$$

In the above equation, $n(\omega)$ and $k(\omega)$ are the real and imaginary part of complex $\tilde{n}(\omega)$. Following Kramers-Kronig relations can be used to describe relation between refractive index $n(\omega)$ and the extinction coefficient $k(\omega)$ [23]:

$$n\,(\omega) = 1 + \frac{2}{\pi} P \int_0^{\infty} \frac{k(\omega')}{\omega' - \omega} d\omega' \tag{6}$$

$$k\,(\omega) = -\frac{2}{\pi} P \int_0^{\infty} \frac{n(\omega') - 1}{\omega' - \omega} d\omega' \tag{7}$$

Extinction coefficient $k(\omega)$ and refractive index $n(\omega)$ can also be described in terms of the calculated values of real part $\varepsilon_1(\omega)$ and imaginary part $\varepsilon_2(\omega)$ of complex dielectric function of the compounds under study [24]:

$$n(\omega) = \left[\frac{\sqrt{\varepsilon_1^2(\omega) + \varepsilon_2^2(\omega)}}{2} + \frac{\varepsilon_1(\omega)}{2} \right]^{1/2} \tag{8}$$

$$k(\omega) = \left[\frac{\sqrt{\varepsilon_1^2(\omega) + \varepsilon_2^2(\omega)}}{2} - \frac{\varepsilon_1(\omega)}{2} \right]^{1/2} \tag{9}$$

Following Peolman relation can be satisfied by the static values of real dielectric function $\varepsilon_1(0)$ and refractive index $n(0)$:

$$n(0) = \sqrt{\varepsilon_1(0)} \tag{10}$$

Calculated spectra of refractive index $n(\omega)$ as a function of incident photon energy is shown in Fig. 5 (c). It can be noted from the spectra of refractive index $n(\omega)$ that the values of zero frequency limit (static values) are approximately 3.6 and 7.6 for Cu_2Se and [Cu_2Se]:Cl, respectively. Highest peaks in the spectra occurs at almost 1.1 and 0.4 eV for Cu_2Se and [Cu_2Se]:Cl, respectively.

One can see the shifting in the curve towards lower energy and also a sharp increase and decrease in the curve of [Cu_2Se]:Cl. Main peaks are present in an energy range of 3.0 to 9.0 eV and 0 to 3.0 eV for Cu_2Se and [Cu_2Se]:Cl, respectively. Threshold value also shifted to below 0 eV for [Cu_2Se]:Cl as compared to Cu_2Se that have threshold value of approximately 0.7 eV.

Highest peaks of extinction coefficient $k(\omega)$ corresponds to approximately 4.5 and 2.2 eV for Cu_2Se and [Cu_2Se]:Cl, respectively.

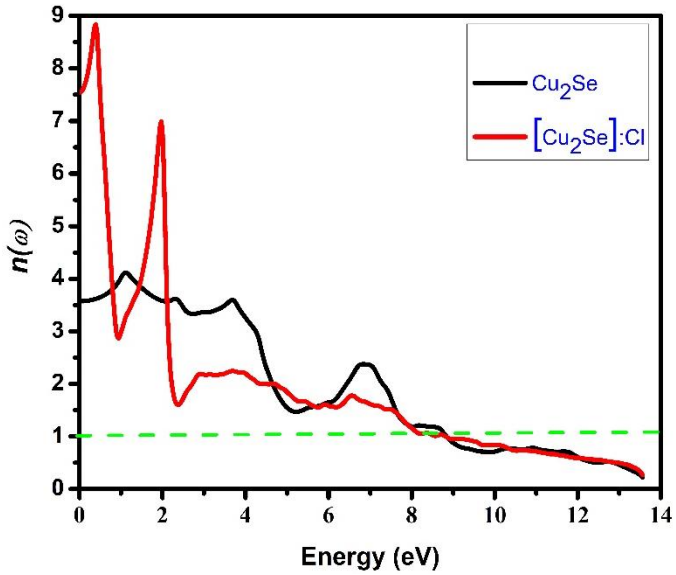

(c)

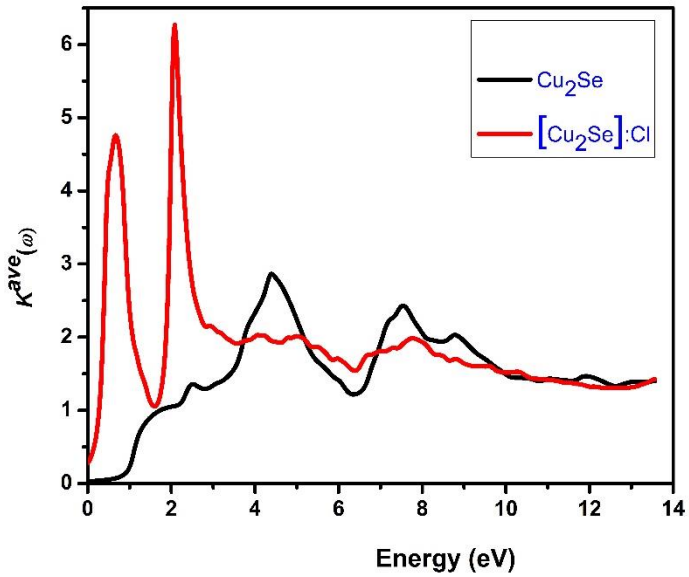

(d)

Reflectivity $R(\omega)$ is another essential parameter to get more insight of the optical transitions of the aforesaid compounds. Calculated values of refractive index $n(\omega)$ and extinction coefficient $k(\omega)$ can be used to calculate reflectivity $R(\omega)$ by using the following relation [24]:

$$R(\omega) = \left|\frac{\tilde{n}(\omega)-1}{\tilde{n}(\omega)+1}\right| = \frac{(1+n)^2+k^2}{(1-n)^2+k^2} \quad (11)$$

Calculated spectra of reflectivity $R(\omega)$ is presented in Fig. 5 (e). Values of reflectivity $R(\omega)$ at zero frequency limit ($R(0)$) are given as approximately 0.21 and 0.59 for Cu_2Se and [Cu_2Se]:Cl, respectively. Static values of reflectivity $R(0)$ shows that these compounds possess semiconducting nature as its values are not around unity.

Optical conductivity $\sigma(\omega)$ and imaginary part $\varepsilon_2(\omega)$ of complex dielectric function are related with each other by following equation [25]:

$$\sigma(\omega) = \frac{\omega}{4\pi}\varepsilon_2(\omega) \quad (12)$$

Absorption coefficient $\alpha(\omega)$ can be defined as the length travelled by photon inside the material while having greater energy than the energy band gap before its complete absorption [22]. Absorption coefficient $\alpha(\omega)$ can be calculated by using real $\varepsilon_1(\omega)$ and imaginary part $\varepsilon_2(\omega)$ of complex dielectric function by using following equation [26]:

$$\alpha(\omega) = \sqrt{2\omega}\left[\sqrt{\varepsilon_1^2(\omega)+\varepsilon_2^2(\omega)} - \varepsilon_1(\omega)\right]^{1/2} \quad (13)$$

Following relation can be used to relate absorption coefficient $\alpha(\omega)$ and extinction coefficient $k(\omega)$ with each other [26]:

$$k(\omega) = \frac{c}{2\omega}\alpha(\omega) \quad (14)$$

Calculated spectra of absorption coefficient $\alpha(\omega)$ is presented in Fig. 5 (f). Threshold value of absorption coefficient $\alpha(\omega)$ is shifted to approximately 0.2 eV for [Cu_2Se]:Cl as compared to Cu_2Se that have threshold value of approximately 1.7 eV. We can note an increase in the spectra of absorption coefficient $\alpha(\omega)$ for both compounds with increasing energies of incident photons. Main peaks in the spectra of both compounds are present in the energy range of 2.0 to 10.0 eV. Cu_2Se shows transparent behavior in infrared region whereas [Cu_2Se]:Cl absorb photons in this region.

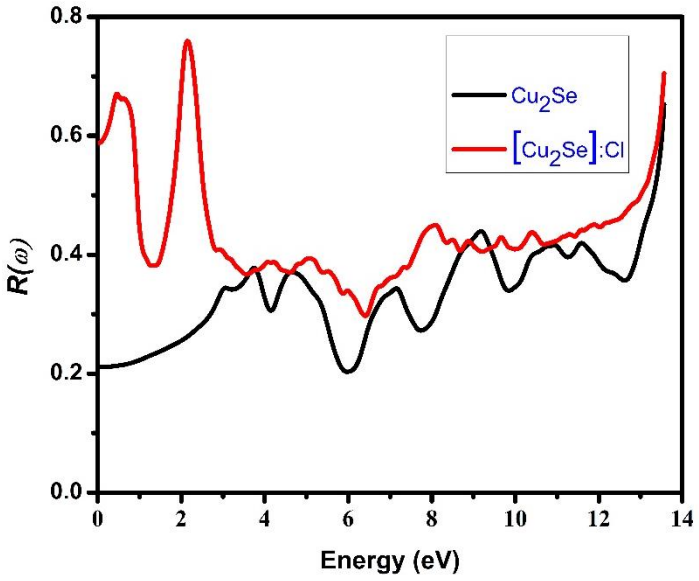

(e)

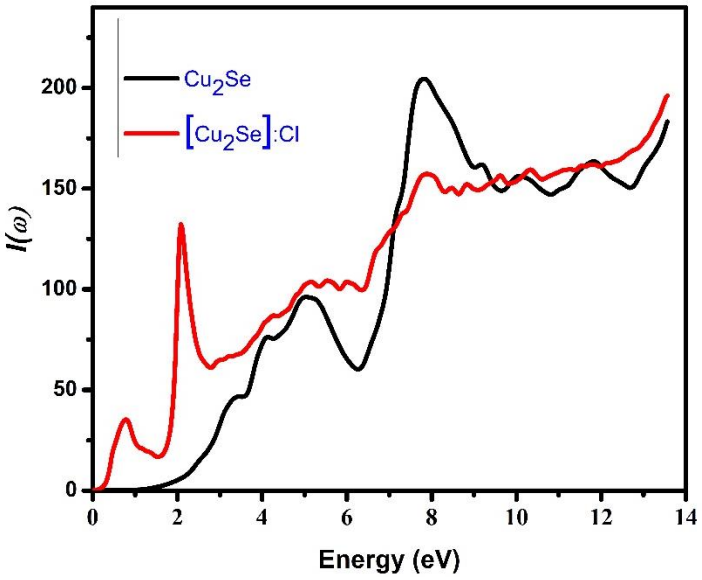

(f)

Energy loss function $L(\omega)$ play an important role in getting information regarding the number of non-scattered and scattered electrons by atoms in the lattice sites and also the energy loss due to it. Energy loss function $L(\omega)$ can be calculated from real $\varepsilon_1(\omega)$ and imaginary part $\varepsilon_2(\omega)$ of complex dielectric function by using the following equation [26]:

$$L(\omega) = -Im\left(\frac{1}{\varepsilon(\omega)}\right) = \frac{\varepsilon_2(\omega)}{\varepsilon_1^2(\omega)+\varepsilon_2^2(\omega)} \quad (15)$$

Equation 15 shows that imaginary part $\varepsilon_2(\omega)$ of complex dielectric function and energy loss function have totally opposite behavior for different energies of photons as they are strongly related with each other. One can notice that energy loss function has minimum values in infrared and visible region as imaginary part $\varepsilon_2(\omega)$ of complex dielectric function is dominant in these regions showing that maximum absorption of photons take place in this region.

Calculated spectra of energy loss function $L(\omega)$ is presented in Fig. 5 (g). Threshold value of energy loss function $L(\omega)$ is shifted to approximately 0.2 eV for [Cu_2Se]:Cl as compared to Cu_2Se that have threshold value of approximately 1.1 eV. Highest peaks are present around 13.0 eV, which means that maximum photons are vanished in upper UV region. For both compounds, multiple peaks are present in the calculated results of energy loss function $L(\omega)$. Highest peak (most energetic) in the spectra of energy loss function $L(\omega)$ corresponds to plasma resonance frequency.

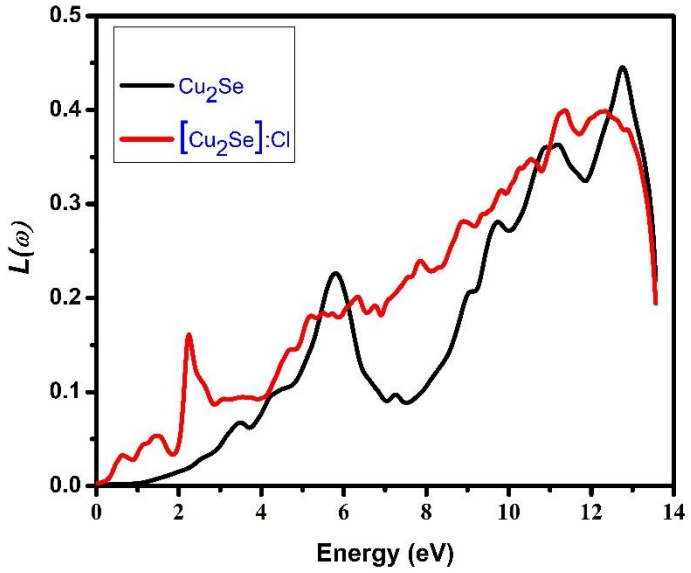

(g)

Fig. 5: Real part ($\varepsilon_1(\omega)$), (b) imaginary part ($\varepsilon_2(\omega)$) of complex dielectric function, (c) refractive index $n(\omega)$, (d) extinction coefficient $k(\omega)$, (e) reflectivity $R(\omega)$, (f) absorption coefficient $\alpha(\omega)$ and (g) energy loss function $L(\omega)$ for Cu_2Se and [Cu_2Se]:Cl

CONCLUSION

The optoelectronic properties of Cl doped Cu2Se were studied using FP-(L)APW method with GGA as exchange-correlation functional. The obtained lattice parameter is in perfect agreement

with the experimental one. mBJ have been used for the prediction of electronic properties. As a result, Cu2Se: Cl is metallic material. The refractive index variations and the different optoelectronic transitions between the top of the valence band and the bottom of the conduction band have been identified by the determination of the dielectric function.

REFERENCES

1. Y. Zhao, C. Burda, Energy Environ. Sci. 5 (2012) 5564.
2. A. Romeo, M. Terheggen, D. Abou-Ras, D.L. Batzner, F.-J. Haug, M. Kalin, D. Rudmann, A.N. Tiwari, Prog. Photovolt. Res. Appl. 12 (2004) 93.
3. H. Liu, X. Yuan, P. Lu, X. Shi, F. Xu, Y. He, Y. Tang, S. Bai, W. Zhang, L. Chen, Y. Lin, L. Shi, H. Lin, X. Gao, X. Zhang, H. Chi, C. Uher, Adv. Mater. 25 (2013) 6607.
4. S.T. Lakshmikumar, Mater. Sol. Cells 32 (1994) 7.
5. H. Okimura, T. Matsumae, R. Makabe, Thin Solid Films 71 (1980) 53.
6. S.C. Riha, D.C. Johnson, A.L. Prieto, J. Am. Chem. Soc. 133 (2011) 1383.
7. L. Kriegel, C. Jiang, J. Rodriguez-Fernandez, R.D. Schaller, D.V. Talapin, E. da Como, J. Feldmann, J. Am. Chem. Soc. 134 (2012) 1583.
8. S. Kashida, W. Shimosaka, M. Mori, D. Yoshimura, J. Phys. Chem. Solids 64 (2003) 2357.
9. M. R asander, L. Bergqvist, A. Delin, J. Phys. 25 (2013) 125503.
10. L. Gulay, M. Daszkiewicz, O.M. Strok, A. Pietraszko, Chem. Met. Alloys 4 (2011) 200.
11. M.C. Nguyen, J.-H. Choi, X. Zhao, C. Wang, Z.Y. Zhang, K. Ho, Phys. Rev. Lett. 111 (2013) 165502.
12. D. Jariwala, V.K. Sangwan, L.J. Lauhon, T.J. Marks, M.C. Hersam, ACS Nano 8 (2014) 1102.
13. G.P. Sorokin, Y.M. Papshev, P.T. Oush, Sov. Phys. Solid State 7 (1966) 1810.
14. G.K. Padam, Thin Solid Films 150 (1987) L89.
15. S.R. Kodigala, Thin Film Solar Cells From Earth Abundant Materials: Growth and Characterization of Cu2(ZnSn)(SSe)4 Thin Films and Their Solar Cells, Elsevier, 2014, p. 116
16. P. Blaha, K. Schwarz, G.K.H. Madsen, D. Kvasnicka, J. Luitz, Wien2k an Augmented Plane Wave Plus Local Orbital Program for Calculating the Crystal Properties, Vienna University of Technology, Austria, 2001.

17. F. Tran, P. Blaha, Phys. Rev. Lett. 102 (2009) 226401–226404.
18. F. Wooten, Optical Properties of Solids, Academic Press, New York, USA, (1972).
19. R. L. Kronig, J. Opt. Soc. Am. 12 (1926) 547-556.
20. H. A. Kramers, AttiCongr. Intern. Fisicas (Transactions of Volta Centenary Congress) 2 (1927) 545-557.
21. D. R. Penn, Phys. Rev. 128 (1962) 2093-2097.
22. M. Fox, Optical Properties of Solids, Oxford University Press (2001).
23. 11N. W. Ashcroft, N. D. Mermin, Solid State Physics, Harcourt Brace College Publishers, New York (1976).
24. 12N. Ullah, G. Murtaza, R. Khenata, K. M. Wong, Z. A. Alahmed, Phase Transitions, 87 (2014) 571-581
25. 13M. Dressel, G. Gruner, Electrodynamics of Solids, Cambridge University Press, Cambridge, (2001).
26. 14F. Ahmadian, A. Salary, J. Korean Phys. Soc. 68 (2016) 227-237.